All-optical tunable delay-line memory based on a semiconductor cavity-soliton laser

M. Eslami and R. Kheradmand*
Photonics Group, Research Institute for Applied Physics and Astronomy, University of Tabriz, Tabriz, Iran

F. Prati
Dipartimento di Scienza e Alta Tecnologia, Università dell'Insubria, Via Valleggio 11, 22100 Como, Italy
(Received 29 October 2013; published 15 January 2014)

Cavity soliton lasers in a vertical-cavity surface-emitting laser with a saturable absorber can spontaneously move provided that a proper ratio of the carrier lifetimes in the amplifier and in the absorber is considered. Use is made of this fact to propose a scheme based on which a tunable all-optical delay line can be demonstrated. This easy-to-realize delay device exhibits high delay range, a very good delay resolution, and a wide extent of available data bandwidth. Also it is shown that the ratio of delay time to pulse duration (fractional delay) can be as large as 2300.

DOI: 10.1103/PhysRevA.89.013818 PACS number(s): 42.55.Px, 42.65.Tg, 42.65.Pc, 42.79.Ta

I. INTRODUCTION

Nowadays the need for higher information capacity demands some kind of buffering or delaying mechanism which is necessary for avoiding the so-called data packet contention. This difficulty has its origin in the fact that switches or routers can only process one packet at a time and problems show up when it comes to the simultaneous arrival of two data packets. The solution is to build a buffer, which places one of the packets on hold while the other clears the switch [1]. This kind of all-optical delay device is also of interest in other fields; optical coherence tomography [2], optical control of phased array antennas for radio-frequency communication [3], and optical sampling and pattern correlation [4], to name a few.

Many methods have been suggested so far to realize an all-optical delay line, the most famous is slow light which is proven to have no fundamental limitations to the maximum fractional pulse delay [5]. However, the fractional delay that has been generated so far in slow-light schemes is usually limited to a few pulse widths. Such schemes include electromagnetically induced transparencies [6,7], coherent population oscillations [8–10], and stimulated Brillouin- or Raman-scattering processes [11–14]. A method based on parametric wavelength conversion and dispersion proved a tunable delay as large as 800 ps for pulses of approximately 10 ps in duration, i.e., 80 pulse widths of delay [15]. Gaeta *et al*. achieved an advancement over a total range of more than 1200 pulse widths in a scheme based on self-phase modulation and dispersion [16].

An alternative approach to an all-optical delay line was introduced using semiconductor cavity solitons [17,18]. A cavity soliton (CS) is a light pixel which forms in an optical resonator containing a nonlinear material. This approach is based on injecting an optical bit stream into an optical resonator, creating cavity solitons that drift transversely with a controllable velocity. The amplitude or phase gradient imposed on the input injection (holding beam) plays the role of a force which removes the already-switched-on CSs from their initial positions and moves them toward the maxima of the gradient. The speed at which the CSs move, hence the delay, depends on the form and strength of the applied gradient and provides the needed amount of delay for the pulse before impinging on the router. However, using amplitude or phase gradients adds technical difficulties to the matter and limits its ease of use in integrated circuits.

In a vertical-cavity surface-emitting laser (VCSEL) with saturable absorber, it has been shown that by proper adjustment of a bifurcation parameter r, which is the ratio of the carrier lifetimes in the amplifier and in the absorber media, CSs can be set to motion hence removing the need for applying gradients through the use of a holding beam. In real experimental conditions one should equivalently use the injection parameter μ, since the value of r is typical of the sample although it can be adjusted with a proper choice of materials in the process of growing the sample [19]. Here, for numerical convenience we have kept μ fixed and varied r. We show that this technique leads to a remarkable capability of delay tuning, besides promising less-complex realization. Also it will be numerically demonstrated that a maximum delay amount of at least 2300 pulse widths are realizable which is approximately twice as large as that reported in Ref. [16].

The sequence of the paper goes as follows: a detailed study of the model employed is in Sec. II, simulation results are in Sec. III, and the conclusion is at the end.

II. MODEL

The dynamics of a VCSEL-based CS laser which contains a saturable absorber is described by the following set of equations [20]:

$$\frac{\partial F}{\partial t} = [(1 - i\alpha)D + (1 - i\beta)d - 1 + i\nabla^2]F, \tag{1}$$

$$\frac{\partial D}{\partial t} = b_1[\mu - D(1 + |F|^2) - BD^2], \tag{2}$$

$$\frac{\partial d}{\partial t} = b_2[-\gamma - d(1 + s|F|^2) - Bd^2]. \tag{3}$$

F is the slowly varying amplitude of the electric field, and D, d are population variables defined as

$$D = \eta_1(N_1/N_{1,0} - 1), \quad d = \eta_2(N_2/N_{2,0} - 1), \tag{4}$$

*r_kheradmand@tabrizu.ac.ir

where N_1 and N_2 are the carrier densities in the active and passive materials, respectively, $N_{1,0}$ and $N_{2,0}$ are their transparency values, and η_1, η_2 are dimensionless coefficients related to gain and absorption, respectively. The parameters α and b_1 (β and b_2) are the linewidth enhancement factor and the ratio of the photon lifetime to the carrier lifetime in the active (passive) material, μ is the pump parameter of the active material, γ is the absorption parameter of the passive material, s is the saturation parameter, and B is the coefficient of radiative recombination. For further details on the essence of the parameters, see Ref. [21]. Time is scaled to the photon lifetime, and space is scaled to the diffraction length. Typically a time unit is a few ps and a space unit $\sim$4 μm.

The values which are used for the defined parameters are $s = 1$, $B = 0.1$, $\alpha = 2$, $\beta = 1$, $b_1 = 0.01$, and $\gamma = 2$. The bifurcation parameter, which is responsible for passing from a stable stationary region to a moving region, is defined as $r = b_2/b_1$. The lasing homogeneous solution is everywhere modulationally unstable because $\alpha > \beta$ [21]. Stable CSs may exist in the interval $4.56 < \mu < 5.18$ where the upper branch coexists with the stable nonlasing solution. However, their stability depends on the parameter r. A necessary condition for the CS to be stable for a given μ is that, for the same μ, the lasing homogeneous solution is stable against a Hopf instability. It was shown that, for the mentioned choice of parameters, this means that it must be $r \leqslant 1.6$–1.7. Stationary states and CS stability discussions can be found in Ref. [19], along with the full description on the drift instability and its properties. The calculations there show that, for $r < 1$ with $b_1 = 0.01$, the drift instability shows up in the interval $4.8 \leqslant \mu \leqslant 5.1$ and $0.65 \leqslant r \leqslant 0.75$. This drift instability makes the CSs to move along straight lines at a fixed speed which grows with distance from the instability threshold and depends on the (μ,r) parameters, accompanied by a reduction in their intensity. For a pump value of $\mu = 5$, it can be shown that the range of the bifurcation parameter capable of giving rise to moving CSs is $0.678 \leqslant r \leqslant 0.711$.

These findings for the CSs in a VCSEL with saturable absorber are used to design a tunable all-optical delay line which can find applications such as buffers in communication systems.

III. RESULTS AND DISCUSSION

The dynamical equations were integrated numerically using a split-step method with periodic boundary conditions. A 128×128 grid is used with a space step $ds = 0.5$, which corresponds to 2 μm. The time unit is the photon lifetime, which here we set equal to 4 ps. A CS can be created by a single pulse of light and remains fixed at the point of addressing in a transversely homogenous system. The duration of this pulse has been shown to be less than 0.25 ns for a successful switching of CSs [22,23]. An amplitude of $F_0 = 8$ and a width of $w = 2$ for the pump current of $\mu = 5$ is used in the Gaussian function of the incoming pulses (bit streams) which is meant to periodically write CSs:

$$F_{\text{inj}}(x,y) = F_0 \exp\{[-(x-x_0)^2 - (y-y_0)^2]/(2w^2)\}, \qquad (5)$$

where we assumed that injection is done at the cavity frequency during an injection time of 0.132 ns. By increasing the amplitude F_0 up to 14 we can reduce the injection time [23], hence further enhancing the fractional delay value, but here we prefer to keep $F_0 = 8$ and the injection time equal to 0.132 ns, which is the minimum duration for successful switching, as shown in Fig. 1.

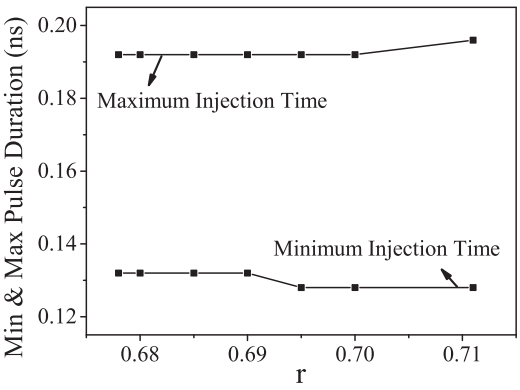

FIG. 1. The range of pulse width that can excite a CS successfully for different r values; the amplitude of the pulse is kept fixed at 8.

To implement a delay-line behavior, the bifurcation parameter r is set to the range for which CSs undergo a moving mechanism, i.e., $0.678 \leqslant r \leqslant 0.711$. The motion is, in nature, in a random direction with a certain rest time depending on the value of r. In order to impose a certain well-defined direction of motion, which is essential for a delay line, and also removing and/or reducing the rest time after which the CS starts moving, the considered model uses a specific shape for the pump current which obeys the function

$$\mu = (\mu_1 + \mu_2)\exp\{[-(x-x_0)^n - (y-y_0)^n]/(w_1)^n\} - \mu_2 \exp\{[-(x-x_0-m)^n - (y-y_0)^n]/(w_2)^n\}, \qquad (6)$$

where the corresponding values are $\mu_1 = 5$, $w_1 = 58$, $w_2 = 56$, $m = 7$, $n = 20$, and m determines the width of the introduced edge and μ_2 its height. The profiles of this pump structure are shown in Fig. 2. To realize this experimentally, some injection engineering techniques have been proposed in Ref. [24], giving the prospect of soliton spatial positioning by exploiting the possibility of applying bias gradients for controlling soliton transverse displacements in broad-area VCSEL devices.

As depicted in Fig. 2, introducing an edge to the pump profile simulates a square pump with ridged boundary in just one side of the square. In such a case, after exciting a CS close to the ridged end of the square pump it will be immediately set to motion by the repulsive act of the boundary, which is in fact reminiscent of current crowding effect. No CSs can be switched on in the ridged area or even very close to it. Actually the reflective property of such ridged boundaries is employed here because they make a reflection point at which the CS path bends when close to it, avoiding any contact. However, there is a key difference in this structure that breaks the symmetry for the CS motion. It was shown that such symmetry makes the CS choose its direction of motion by chance in the presence of a pump with circular or square boundaries on all sides of the square [19,25]. Here the situation is different due to the single ridged boundary which clearly dictates a well-defined

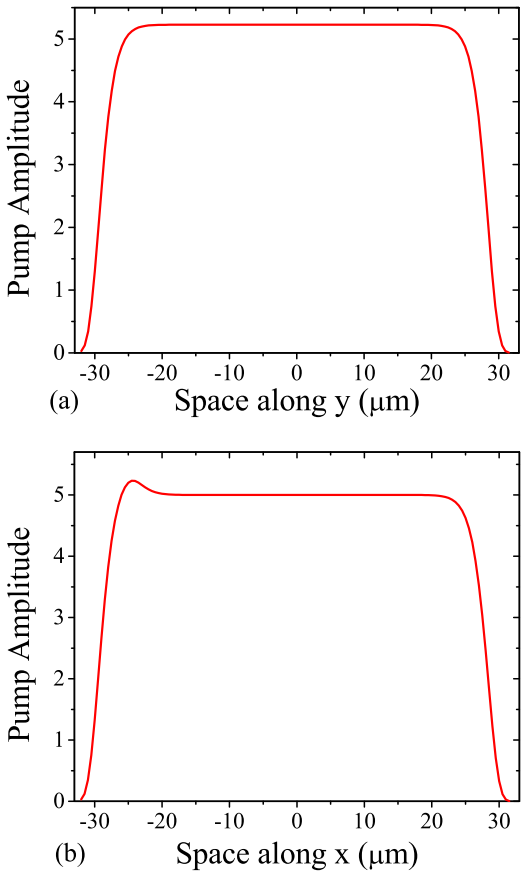

FIG. 2. (Color online) Pump profile along two perpendicular axes crossing at the center of the VCSEL. The pump is uniform along the vertical axis (y) and displays an edge in the horizontal axis (x), which is meant to force the motion of the CS along the positive x direction. CSs are positioned initially in $x = -21.5$, $y = 0$.

path of motion, heading from the ridged edge directly to the other end.

An alternative way to fix the direction of motion would be to inject a weak address pulse in the vicinity of the CS [22]. This very short pulse attracts or repels the CS, hence dictating a desired direction. However, this can add another complexity in real situations while the proposed edge-in-pump profile eliminates any need of secondary address pulses.

The repelling force from the edge also removes the rest time typical of this kind of motion and there is virtually no such a delay due to the rest time for higher edges. It should be said that the height of the ridged end and also its width determine the velocity of the motion as well as the amount of reduction in the rest time. So, it is possible to adjust the velocity at which the CSs move in the delay line according to need. We note that, for higher values for the edge, no CS can survive, although the motion is faster in the beginning. Figure 3 shows the CS velocity for different r values and edge heights μ_2. In fact, what we plot is the average velocity calculated along the whole path starting from the start of motion. The corresponding reduction in rest time due to the edge height is also shown.

Note that the CSs are excited periodically at a rate determined by the minimum distance that the CSs can have from each other, i.e., 25 grid points. Hence the velocity of CS motion

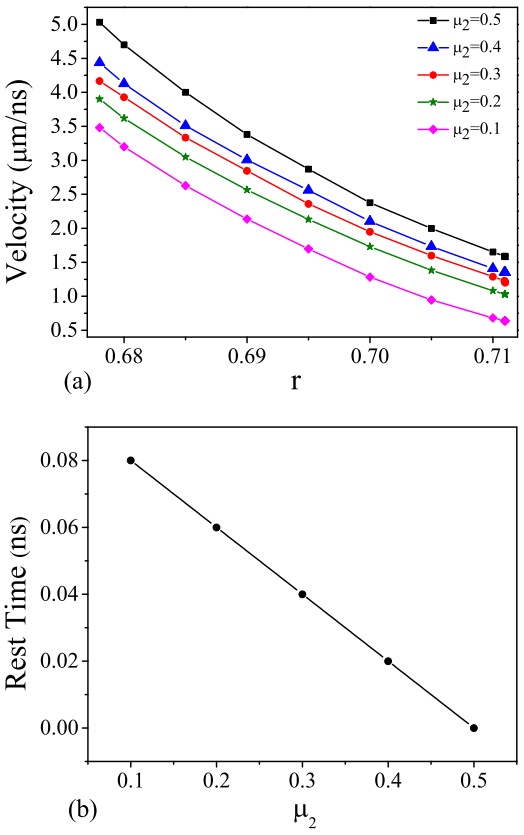

FIG. 3. (Color online) (a) Velocity of an already-established CS versus the value of bifurcation parameter r. (b) Reduction in the rest time of CS after which it starts moving, for different heights of the edge.

determines how fast other CSs can be sequentially written one after another. We can define a data transmission rate which actually corresponds to the inverse of the minimum-required delay between successive switching. Figure 4 shows the data transmission rate for various edge heights and values of r. In fact this rate is limited by the minimum possible distance that CSs can have before interacting.

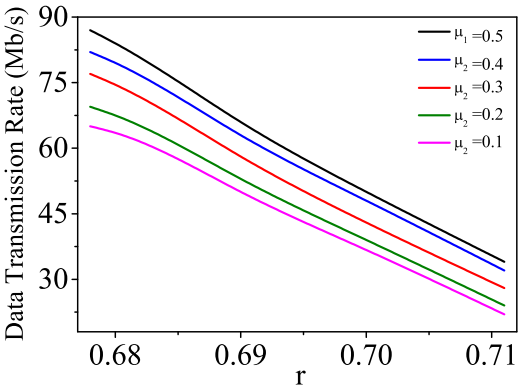

FIG. 4. (Color online) Data transmission rate for different μ_2 and r. Each CS is considered to represent one single bit of information. The rate is also a manifestation of minimum distance available between successive CSs.

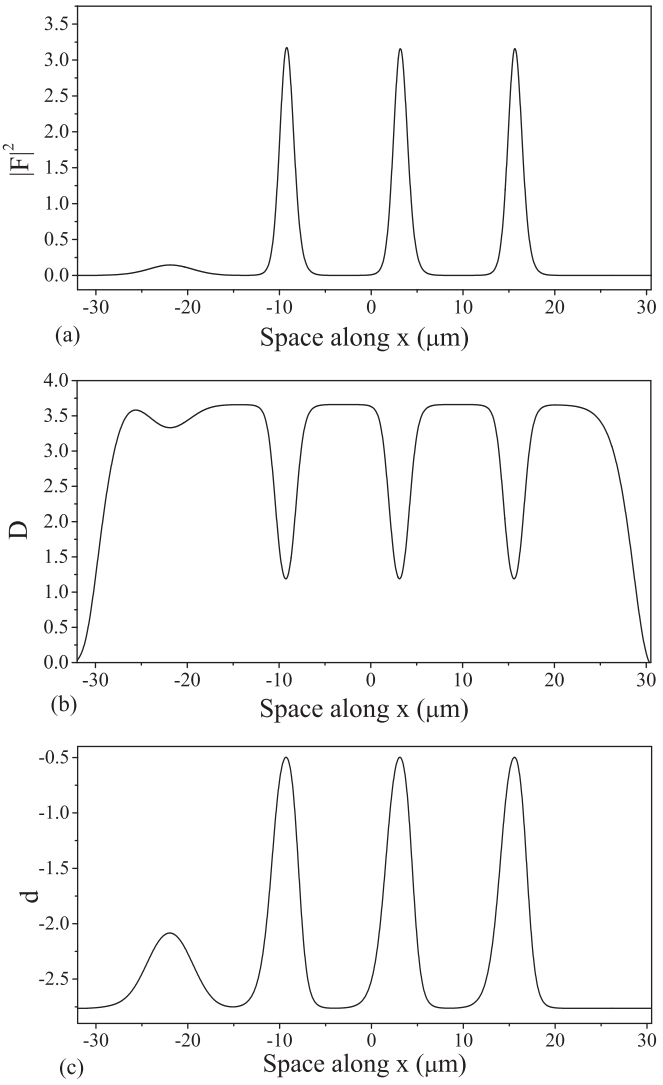

FIG. 5. (a) Profiles of field intensity of the populations (b) D and (c) d. It is clear that the tails of CSs do not interact. The slight peakon the left side of the graphs belongs to the edge in the pump shape.

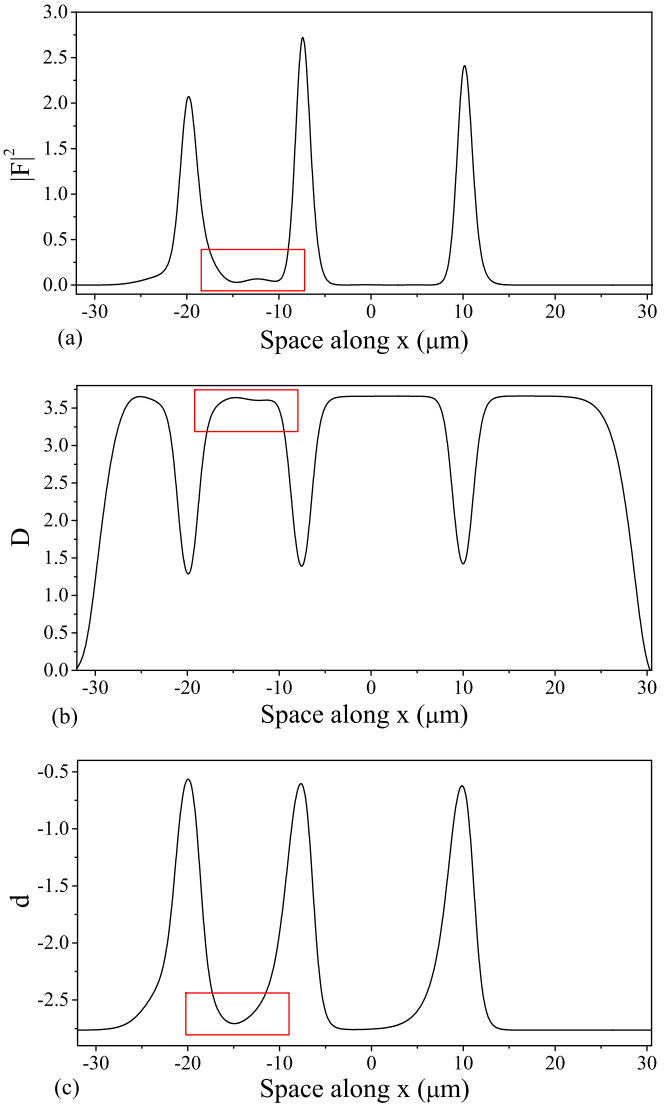

FIG. 6. (Color online) Overlapping of tails of CSs, right after the arrival of the third pulse, which leads to their destruction. Profiles of (a) field population in (b) amplifier and in (c) absorber media.

Figure 5 shows the profile of CSs which are written in a line by satisfying the criteria of 25 grid points of distance, which is equal to 50 μm corresponding to 6.25 CS diameters [full width at half maximum (FWHM) of the CSs is approximately 8 μm]. As can be seen, there is no overlap of tails of the CSs. For $\mu_2 = 0.5$ and $r = 0.678$ one must set the time interval between incoming pulses to 11.4 ns in order to allow CSs move from their initial positions by 50 μm. In contrast, in Fig. 6 it is depicted that, when the time interval between CSs is slightly shorter than the minimum value, here 11.32 ns, tail interactions take place, the cost of which is to ruin the CSs.

Up to now, various all-optical delay lines have been proposed in different systems, therefore there is a need for some metrics to make an approximate comparison. In what follows some metrics are defined against which the efficiency of the proposed device can be evaluated.

(1) Maximum delay: The maximum achievable delay value in this system can be obtained by considering the maximum possible value for the ratio r which is 0.711 and tuning the height of the edge to the minimum value of $\mu_2 = 0.1$. This set of parameter values proves a maximum delay (or the slowest motion of the CSs) of the system to be 312.45 ns. It should be noted that the maximum delay value is calculated based on the fact that the considered device size (pumped area) in simulations is about 200 μm, which is consistent with experiments, and the typical pulse speed in fibers delivering the pulse to the device is 200 μm/ns. So, the same pulse would pass the device length in 1 ns if there were no delaying device.

(2) Delay range: The tuning range (from minimum to maximum) that the delay can achieve is wide, thanks to the two effective parameters involved in tuning the speed of CSs in the device (μ_2,r). The fastest achievable motion of the CS is 5.031 μm/ns and the slowest is 0.638 μm/ns; thus, according to the above discussion for calculating the delay value, the delay range can vary from 38.75 to 312.45 ns.

(3) Delay resolution: The minimum incremental delay tuning step is 0.48 ns which is calculated for $\Delta r = 2 \times 10^{-5}$

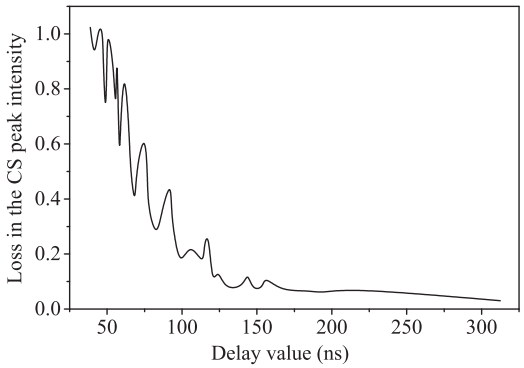

FIG. 7. Reduction in the CS peak intensity as a result of different delay values. Note that the intensity of a CS at rest is almost 3.63 (arb. units) and, as its speed increases, it experiences more reduction in intensity.

and edge height of $\mu_2 = 0.1$. It is worth noting that the mentioned value for Δr is the minimum possible for which sensible change in the velocity of the CSs can occur.

(4) Loss over delay: It is well known from previous works that a moving CS will experience some reduction in its peak intensity [19]. So, the amount of loss incurred per unit delay can be calculated using the fact that the intensity of a CS at rest is about 3.63 (arb. units) and the motion of CS would reduce this value depending on how fast the displacement is. Thus, the minimum incremental delay which is achievable by using $\Delta r = 2 \times 10^{-5}$ reduces the CS peak intensity from its rest value of 3.63 (arb. units) by 0.11×10^{-3}. That is, each delay unit imposes a loss of about 0.11×10^{-3} in the intensity of the CS. The corresponding loss for different delay values is shown in Fig. 7.

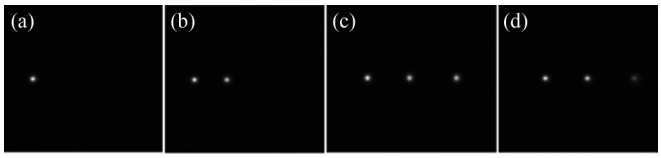

FIG. 8. The sequence of CSs in the delay line as they are written and read. Each picture, which is taken from simulations, leads the previous by 11.4 ns, satisfying minimum distance of 25 grid size. Values are $\mu_2 = 0.5$ and $r = 0.678$.

In Fig. 8, the sequence of successive CS writing and their motion in the line are shown. As is clear, CSs are read at the end of the line clearing the place for other bits of information. Additional channels can be added laterally provided that the minimum distance condition is fulfilled. In this way, the capacity of the delay line can be dramatically increased.

IV. CONCLUSION

Using the spontaneous motion of CSs in a VCSEL with saturable absorber and by adjusting the joint effective parameter values of (μ_2,r), a highly tunable all-optical delay line is proposed. This scheme has some advantages over previously introduced methods of delaying bit streams in several key factors. Among these are a considerably high delay resolution, extended range of tunability, wide achievable delay range and, most important of all, a very high fractional delay of 2300. Due to an adjustable range of incoming pulse durations that are capable of writing CSs, by tuning the amplitude of the pulse, this device is applicable in an acceptable range of pulse lengths. The loss-over-delay parameter is also numerically calculated which shows more loss when the speed of data transmission is higher.

[1] R. W. Boyd, D. Gauthier, and A. L. Gaeta, Opt. Photonics News **17**, 18 (2006).
[2] E. Choi, S. Y. R. J. Na, G. Mudhana, and B. H. Lee, Opt. Express **13**, 1334 (2005).
[3] J. L. Corral, J. Marti, J. M. Fuster, and R. I. Laming, IEEE Photonics Technol. Lett. **9**, 1529 (1997).
[4] R. Ramaswami and K. N. Sivarajan, *Optical Networks: A Practical Perspective* (Morgan Kaufmann, San Francisco, 2002).
[5] R. W. Boyd, D. J. Gauthier, A. L. Gaeta, and A. E. Willner, Phys. Rev. A **71**, 023801 (2005).
[6] L. V. Hau, S. E. Harris, Z. Dutton, and C. H. Behroozi, Nature (London) **397**, 594 (1999).
[7] M. M. Kash, V. A. Sautenkov, A. S. Zibrov, L. Hollberg, G. R. Welch, M. D. Lukin, Y. Rostovtsev, E. S. Fry, and M. O. Scully, Phys. Rev. Lett. **82**, 5229 (1999).
[8] M. S. Bigelow, N. N. Lepeshkin, and R. W. Boyd, Phys. Rev. Lett **90**, 113903 (2003).
[9] P. C. Ku, F. Sedgwick, C. J. Chang-Hasnain, P. Palinginis, H. W. T. Li, S. W. Chang, and S. L. Chuang, Opt. Lett. **29**, 2291 (2004).
[10] M. van der Poel, J. Mrk, and J. Hvam, Opt. Express **13**, 8032 (2005).
[11] Y. Okawachi, M. S. Bigelow, J. E. Sharping, Z. Zhu, A. Schweinsberg, D. J. Gauthier, R. W. Boyd, and A. L. Gaeta, Phys. Rev. Lett. **94**, 153902 (2005).
[12] K. Y. Song, M. G. Herraez, and L. Thevenaz, Opt. Express **13**, 82 (2005).
[13] J. E. Sharping, Y. Okawachi, and A. L. Gaeta, Opt. Express **13**, 6092 (2005).
[14] Y. Okawachi, M. A. Foster, J. E. Sharping, A. L. Gaeta, C. Xu, and M. Lipson, Opt. Express **14**, 2317 (2006).
[15] J. E. Sharping, Y. Okawachi, J. van Howe, C. Xu, Y. Wang, A. E. Willner, and A. L. Gaeta, Opt. Express **13**, 7872 (2005).
[16] Y. Okawachi, J. E. Sharping, C. Xu, and A. L. Gaeta, Opt. Express **14**, 12022 (2006).
[17] C. McIntyre, A. M. Yao, G.-L. Oppo, F. Prati, and G. Tissoni, Phys. Rev. A **81**, 013838 (2010).
[18] F. Pedaci, S. Barland, E. Caboche, P. Genevet, M. Giudici, J. R. Tredicce, T. Ackemann, A. J. Scroggie, W. J. Firth, G.-L. Oppo, G. Tissoni, and R. Jager, Appl. Phys. Lett. **92**, 011101 (2008).
[19] F. Prati, G. Tissoni, L. A. Lugiato, K. M. Aghdami, and M. Brambilla, Eur. Phys. J. D **59**, 73 (2010).

[20] F. Prati, P. Caccia, G. Tissoni, L. A. Lugiato, K. M. Aghdami, and H. Tajalli, Appl. Phys. B **88**, 405 (2007).
[21] M. Bache, F. Prati, G. Tissoni, R. Kheradmand, L. A. Lugiato, I. Protsenko, and M. Brambilla, Appl. Phys. B **81**, 913 (2005).
[22] H. Vahed, F. Prati, H. Tajalli, G. Tissoni, and L. A. Lugiato, Euro. Phys. J. D **66**, 148 (2012).
[23] K. M. Aghdami, F. Prati, P. Caccia, G. Tissoni, L. A. Lugiato, R. Kheradmand, and H. Tajalli, Euro. Phys. J. D **47**, 447 (2008).
[24] T. Camps, V. Bardinal, E. Havard, M. Conde, C. Fontaine, G. Almuneau, L. Salvagnac, S. Pinaud, and J. B. Doucet, Eur. Phys. J. D **59**, 53 (2010).
[25] F. Prati, L. A. Lugiato, G. Tissoni, and M. Brambilla, Phys. Rev. A **84**, 053852 (2011).